098643

LA-UR-05-5371

Approved for public release; distribution is unlimited

Title: ASSESSING WIND EROSION AS A CONTAMINANT TRANSPORT MECHANISM FOR THE TA-54 MATERIAL DISPOSAL AREA G PERFORMANCE ASSESSMENT AND COMPOSITE ANALYSIS

Author(s): Jeffrey J. Whicker
David D. Breshears

Submitted to: U.S. Department of Energy

Los Alamos
NATIONAL LABORATORY

Los Alamos National Laboratory, an affirmative action/equal opportunity employer, is operated by the University of California for the U.S. Department of Energy under contract W-7405-ENG-36. By acceptance of this article, the publisher recognizes that the U.S. Government retains a nonexclusive, royalty-free license to publish or reproduce the published form of this contribution, or to allow others to do so, for U.S. Government purposes. Los Alamos National Laboratory requests that the publisher identify this article as work performed under the auspices of the U.S. Department of Energy. Los Alamos National Laboratory strongly supports academic freedom and a researcher's right to publish; as an institution, however, the Laboratory does not endorse the viewpoint of a publication or guarantee its technical correctness.

Form 836 (8/00)

31163

Table of Contents

List of Figures i
List of Tables ii
Acronyms and Abbreviations iii
Acknowledgements iv

1.0 Introduction 1
2.0 Methods 3
  2.1 Selection of Measurement Sites 3
  2.2 Measurements 3
    2.2.1 Horizontal Mass Flux Measurements 6
    2.2.2 Vertical Mass Flux Measurements 9
  2.3 Statistical Analyses 11
3.0 Results 12
4.0 Discussion 22
  4.1 Significance of Results 22
  4.2 Qualifications 23
5.0 References 27

List of Figures

Figure 1 Grass and Forb Cover at MDA J Analog Site 4
Figure 2 Piñon-Juniper Cover at TA-51 Analog Site 5
Figure 3 Field Dust Collector with Rotating Samplers at Three Heights 7
Figure 4 Circular Arrangement of Field Dust Samplers 8
Figure 5 Sonic Anemometer for Measuring Wind Velocity 10
Figure 6 Horizontal Mass Flux at Grassland and Woodland Analog Sites over Time (1 m sampling height) 15
Figure 7 Horizontal Mass Flux at Grassland and Woodland Analog Sites (all sampling heights) 16
Figure 8 Wind Velocities at Grassland and Woodland Analog Sites (1 m sampling height) 17
Figure 9 Horizontal Mass Flux at Inward- and Outward-Facing Samplers at Both Analog Sites 18
Figure 10 Estimated Vertical Mass Flux Collected during All Sampling Periods (1 m sampling height) 20
Figure 11 Pre- and Post-Thinning Dust Concentrations at TA-54 Meteorological Station 25
Figure 12 Weekly Flux Gradient Measurements at TA-54 before and after Nearby Thinning Operations 26

List of Tables

Table 1 Summary Statistics for Horizontal Mass Flux Measurements from All Sampling Periods 13
Table 2 Summary Statistics for Horizontal Mass Flux Measurements from Periods without Precipitation 14
Table 3 Summary Statistics for Aerosol Mass Concentration and Vertical Mass Flux at MDA J..... 21

Acronyms and Abbreviations

BSNE	Big Spring Number Eight (dust sampler)
LANL	Los Alamos National Laboratory
MDA	Material Disposal Area
TA	Technical Area
TSP	Total suspended particulate

Acknowledgements

The authors would like to acknowledge the able field assistance of Johnny Salazar, Marvin Gard, and Leo Martinez. They overcame many obstacles to get the job done.

1.0 Introduction

Recent evaluations of landfill performance at Material Disposal Area (MDA) G at Los Alamos National Laboratory (LANL) have highlighted the need to more rigorously consider erosional processes that could impact landfill covers through time. Wind erosion at MDA G is of particular concern for both operational and long-term performance issues associated with covers. Nevertheless, there is a lack of site-specific wind erosion data needed to estimate and project soil loss and contaminant transport rates.

Landfill covers in semiarid settings may be particularly vulnerable to surface erosion because, in general, the limited amount of precipitation does not allow a homogeneous vegetation cover to develop. Hence, these areas often have significant patches of unprotected or bare soil, which are subject to increased soil erosion. Most erosion studies of landfill covers have focused on water erosion. However, recent studies in semiarid landscapes have shown that wind erosion and transport can be substantial (Whicker et al., 2002; Breshears et al., 2003). For example, in a study of three different semiarid ecosystems (shrubland, woodland, and grassland), Breshears et al. (2003) note that long-term wind erosion rates exceeded water erosion rates by approximately 33 times at the shrubland site and 5 times at the woodland site, although water erosion rates at the grassland site were about 3 times greater than wind erosion rates because of the high clay content of the soils. The results of the Breshears et al. study also show that horizontal transport by wind was greater than that by water for all three ecosystems, especially for the shrubland environment. These and other results indicate that wind erosion could affect the long-term integrity of landfill covers and be an important mechanism for the redistribution of surficial contamination at a landfill site (Anspaugh et al., 1975; Sehmel, 1980; Arimoto et al., 2002).

In a broad sense, wind-driven soil movement can be thought of as having two directional components:

- *Mass horizontal transport* is a process in which larger soil particles (generally greater than 50 μm [2.0×10^{-3} in.] in diameter) are transported in a horizontal direction by saltation. The particles remain close to the ground (e.g., at a height of less than 1 m [3.3 ft]) and the process is generally indicative of local soil redistribution (Stout and Zobeck, 1996; Gillette et al., 1997).

- *Mass vertical transport* (e.g., vertical dust movement at a height of more than 1 m [3.3 ft]) suggests long-distance transport of smaller soil particles (generally less than 50 μm [2.0×10^{-3} in.] in diameter). These small particles can be transported into an area (deposition) or removed from an area (net loss).

Vegetation changes through time are important considerations in assessing future wind erosion rates. First, vegetation cover on landfills is likely to undergo successional processes resulting in changes in cover type, coverage, and structure. These changes are expected to impact wind erosion rates; therefore, it is important to quantify the influence of vegetation changes on wind erosion. Second, in addition to the effect of normal vegetation succession, it is important to consider environmental disturbances that may reduce vegetation cover and thus result in significantly increased soil erosion (Fryrear, 1985). Decreases in the amount of ground cover can be particularly dramatic following disturbances such as drought and fire, and can lead to increased wind and water erosion (Davenport et al., 1998; Whicker et al., 2002).

The objective of this study was to provide initial estimates of wind erosion for MDA G through (1) the installation of equipment and collection of wind erosion data at two analog study sites and (2) the development of site-specific wind erosion projections based on collected data. The two analog sites are on Mesita del Buey, to the west of MDA G. The first, located at MDA J, was selected for study because it is representative of the surface soil and vegetative conditions that are expected to prevail at MDA G immediately following closure of the facility. The second site, a piñon-juniper woodland located at Technical Area (TA) 51, was selected because it is expected to represent the type of vegetation that will be present at MDA G after the site has undergone successional changes. Measurements were taken at these two analog sites, rather than directly at MDA G, because ongoing operations at MDA G (such as soil transportation and heavy truck use) would likely mask any wind erosion that would occur in the absence of these activities.

Detailed wind erosion measurements at MDA J included evaluations of vertical and horizontal flux as a function of micrometeorological conditions and particle-size distribution. Horizontal flux measurements were made at TA-51 to address the effects that successional changes in vegetation and soil cover may have on erosional processes at MDA G. This report provides the methodology used to conduct and analyze the measurements, the results obtained from both analog sites (MDA J and TA-51), and projections of annual wind erosion rates.

2.0 Methods

Specific tasks covered by this study included the selection of analog sites, installation of measuring devices and collection of samples, and analysis of field data. This section describes the methodology used to perform these tasks. Section 2.1 focuses on why and how measurement sites were selected, Section 2.2 explains how measurements were made, and Section 2.3 describes how the statistical analysis was performed.

2.1 Selection of Measurement Sites

Erosion measurements were conducted at two surrogate or analog sampling sites located near (i.e., within a couple of kilometers of) MDA G. The first site, MDA J, is characterized as grassland (Figure 1), which is likely to be the first successional stage experienced by MDA G immediately following closure. The second site, located at TA-51 (Figure 2), is a piñon-juniper woodland, which represents a later possible successional state for MDA G. To limit spatial variability in the dust flux measurements, each of the sampling sites was located on top of the same mesa as MDA G and at a similar elevation.

Site selection was based on several important criteria. First, both sites were relatively flat (slopes less than 10 percent) with vegetative cover that was relatively homogeneous in all directions for at least 50 m (160 ft), especially in the prevailing upwind directions. Second, the sites were as far away as possible from roads or other recently disturbed soil surfaces that could produce unusual amount of dust. Third, these sites were expected to be reasonably representative of the likely ground cover that MDA G will experience during early and late stages of succession following its closure and final remediation.

2.2 Measurements

Once representative analog sites were selected, measurements were obtained to quantify the horizontal mass flux of wind-driven dust at both the MDA J and TA-51 sites. Measurements were also obtained at the MDA J site to quantify the vertical dust flux. Sections 2.21 and 2.2.2 discuss how horizontal and vertical mass flux measurements were obtained.

Figure 1
Grass and Forb Cover at MDA J Analog Site

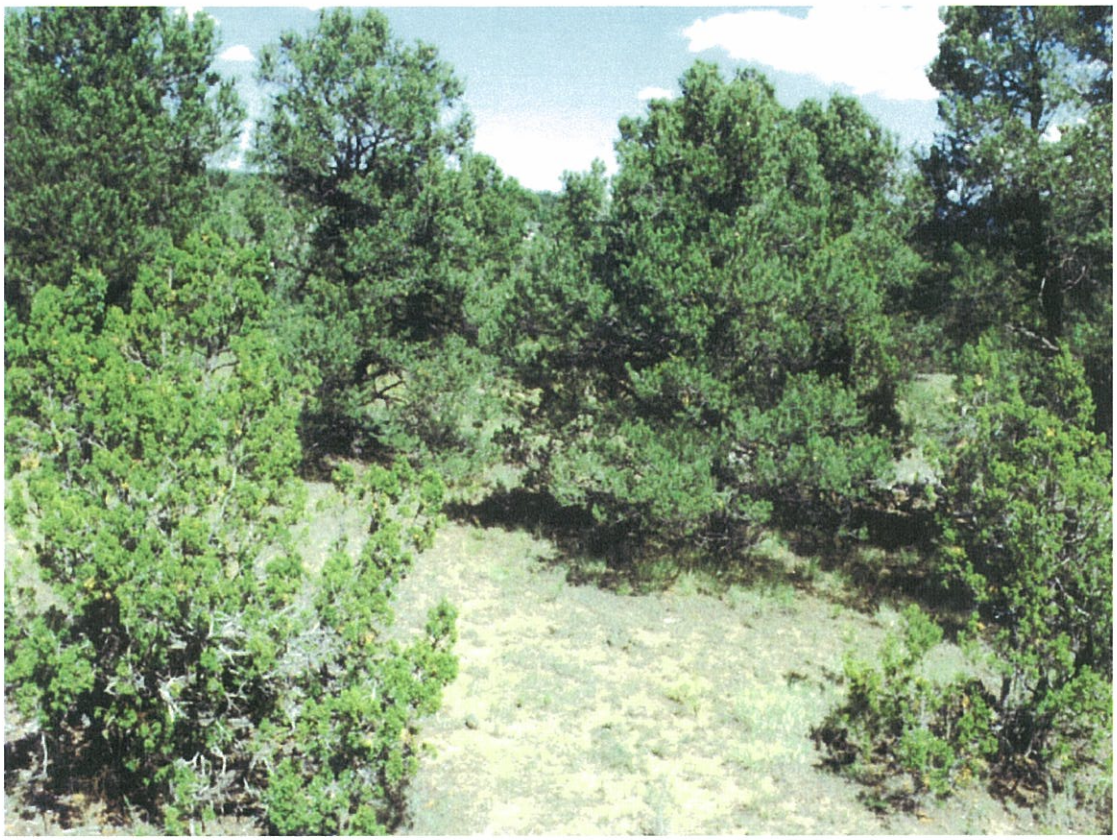

Figure 2
Piñon-Juniper Cover at TA-51 Analog Site

2.2.1 Horizontal Mass Flux Measurements

Wind erosion rates at the two sites were quantified using numerous Big Spring Number Eight (BSNE) samplers (Figure 3). These samplers are passive collectors of airborne dust that have been extensively tested and show good sampling efficiency for soils with higher fractions of sand and silt (Fryrear, 1986; Goossens and Offer, 2000) such as those that are abundant at LANL (Nyhan et al., 1978). These samplers can be assembled easily and inexpensively from interchangeable parts and do not require electricity to operate; thus, numerous samplers can be employed and great flexibility can be used in their placement. Because of this, it was possible to obtain continuous measurements using multiple samplers at multiple sites.

As shown in Figure 3, a fully rotating BSNE sampling station has three samplers operating at heights of 25 cm, 50 cm, and 1 m (10, 20, and 39 in.). This configuration provided measures of integrated resuspension that were generally collected over one- to two-week sampling intervals. The horizontal mass flux was calculated as follows:

$$F_H = \frac{m}{t \times a} \qquad 1$$

Where

F_H = horizontal mass flux (g/m^2/d)
m = mass of the material collected during sampling (g)
t = number of sampling days
a = sampling area (10 cm^2 [1.6 in.^{2}])

Big Spring Number Eight samplers are designed to rotate 360° to allow them to sample wind-blown dust from any direction. This provides a measure of dust flux integrated over all sampling directions. The arrangement of BSNE samplers for this study is shown in Figure 4. To measure total dust flux, four rotating BSNE sampling stations were placed 20 m (65 ft) apart along the east-west and north-south axes of each sampling area.

The net horizontal dust flux was determined at each measurement site by using eight pairs of BSNE samplers positioned 20 m (65 ft) from the center of a circular sampling area at a height of 50 cm (20 in.) (Figure 4); the range of movement of these samplers was restricted to 45°. Each pair consisted of one sampler facing toward the center of the circle and one facing 180° in the opposite direction, away from the center of the circle. Because the collection efficiency of the BSNE samplers is less than 10 percent for off-angle sampling (Fryrear, 1986), each of the eight pairs of motion-restricted collectors sampled wind-blown dust for a different 45° angle from the center point (yielding a combined total of 360° for all eight pairs of inward- and outward-facing samplers). Using these measurements, the net dust flux in the sampling area was calculated as the difference in the amount of dust collected in the inward- versus the outward-facing samplers.

Figure 3
Field Dust Collector with Rotating Samplers at Three Heights

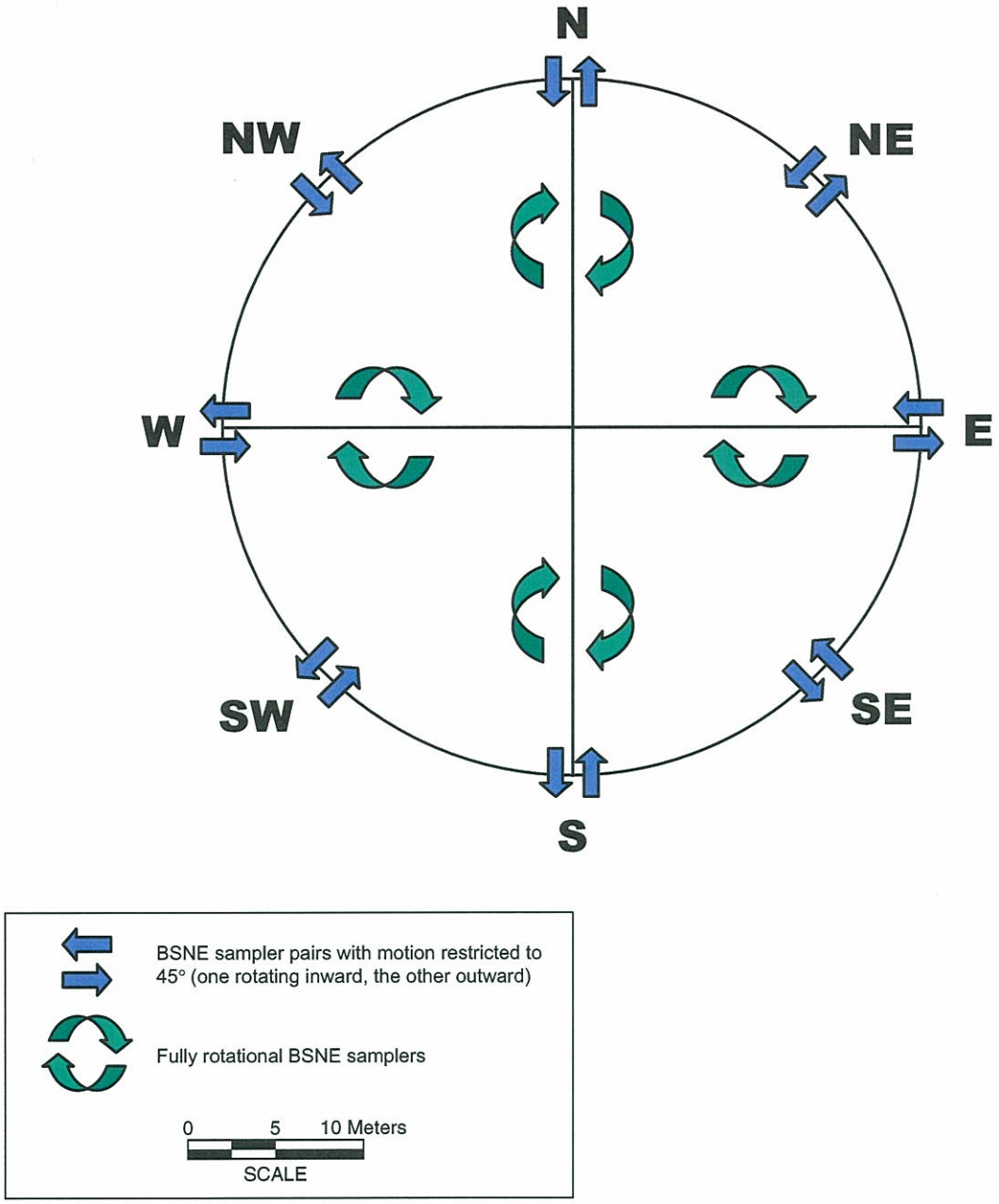

Figure 4
Circular Arrangement of Field Dust Samplers

2.2.2 Vertical Mass Flux Measurements

Vertical flux measurements are primarily a measure of the suspended mass of particles passing through the sampled area during the given sampling time. Resuspension rates are estimated using the meteorological flux gradient method (Stull, 1988):

$$F = K_z \frac{d\chi}{dz} \qquad 2$$

Where

F = vertical mass flux
K_z = eddy diffusivity coefficient
$d\chi/dz$ = differential mass air concentration (χ) with height (z)

The eddy diffusivity coefficient is a linear function of the friction velocity (u_*). The friction velocity is a measure of the boundary shear created as winds pass over vegetation and soils. The friction velocity for a given terrain and wind velocity can be obtained by measuring the wind velocity profile with height (Bagnold, 1941) or it can be determined with highly frequent three-dimensional measurements of wind velocities (Stull, 1988) using Equation 3:

$$u_*^2 = \left[\overline{u'w'}^2 + \overline{v'w'}^2 \right]^{\frac{1}{2}} \qquad 3$$

Where

u' = instantaneous wind velocity component in horizontal direction x (m/s)
v' = instantaneous wind velocity component in horizontal direction y (m/s)
w' = instantaneous wind velocity component in vertical direction z (m/s)

The instantaneous wind velocity components were measured using a sonic anemometer (Campbell Scientific Model CSAT3) (Figure 5), and used to calculate an average friction velocity for each sampling period. In addition, data for the wind profiles with height (as well as other meteorological conditions) were obtained from meteorological stations that were approximately centered within the sampling plots. Once the vertical mass flux (F) was determined, the resuspension rate was calculated by dividing that flux by the density of the local soil and the depth of the resuspendable soil (e.g., 3 mm [0.12 in.]) (Webb et al., 1997).

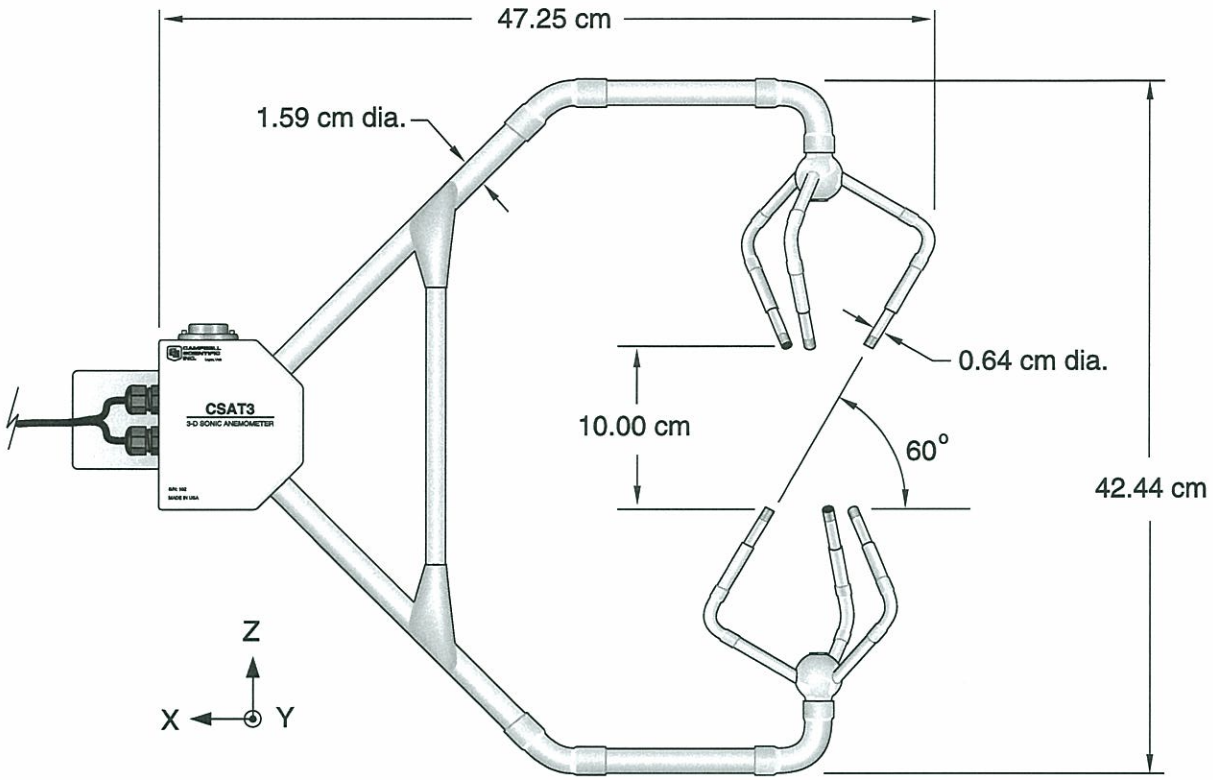

Figure 5
Sonic Anemometer for Measuring Wind Velocity

Source: Campbell Scientific, 2004

To determine the concentration gradient with height ($d\chi/dz$), which is needed for resuspension rate measurements, total suspended particulate (TSP) measurements were made each week. Samplers were placed at heights of 1 and 3 m (3.3 and 9.8 ft) to measure the concentration gradients. The concentration difference ($d\chi$) was calculated as the difference between the mass concentrations at 1 and 3 m (3.3 and 9.8 ft), and the height (dz) was the 2 m (6.6 ft) vertical separation between samplers. The sampling inlet on the TSP air samplers used for this study is slightly modified from the inlet in the sampler described by Liu and Pui (1981), which had an aspiration efficiency of 100 percent (±10 percent) for particles with aerodynamic diameters of 8.5 and 11 μm (3.0×10^{-4} and 4.0×10^{-4} in.) and wind speeds up to 2.5 m/s (8.2 ft/s). While these wind speeds are typical velocities measured at LANL, measurements of resuspension at higher velocities were also needed. Because of this, and the fact that the original Liu and Pui inlet design was for sampling particulate matter with diameters of 10μm (4.0×10^{-4} in.) or less, modifications were made that included placing the filter close to the bottom plate and adding a coarse wire screen to keep insects out of the filter. These changes to the inlet allow sampling without directional dependence, and permit accurate sampling over a wider range of wind velocities and particulate size.

Rodgers et al. (2000) tested the sampler with the modified inlet at wind velocities of 12, 15, and 17 m/s (39, 49, and 56 ft/s), for aerodynamic particle diameters of 5, 10, and 30 μm (2.0×10^{-5}, 3.0×10^{-5}, and 1.0×10^{-4} in.) to determine sampling efficiencies at higher wind velocities. Results of this study suggested that the collection efficiency of the modified inlet was more affected by particle size than by wind velocity. For example, the collection efficiency for the 5-μm (2.0×10^{-5}-in.) diameter particles was about 120 percent (20 percent over sampling, on average) while the collection efficiency dropped to around 50 percent for both the 10- and 30-μm (3.0×10^{-5} and 1.0×10^{-4}-in.) diameter particles.

2.3 Statistical Analyses

Parametric and nonparametric summary statistics for horizontal and vertical fluxes were calculated using SYSTAT® software. The nonparametric Mann-Whitney test was used to test for statistical differences in horizontal flux between grassland and woodland sites and also between inward and outward directional fluxes within each sampling site. Statistical testing for differences between the two sites was performed separately for each sampling height. Attempts were made to limit the potential for soil collection in the BSNE samplers from rainsplash by collecting most of the samples at heights greater than 50 cm (20 in.); even so, the data suggested that rainsplash slightly increased the soil mass collected in our samplers. To compensate, statistical analyses were performed for periods with and without precipitation. Including fluxes measured during periods of precipitation provided higher (more conservative) estimates of mean and standard deviations, but did not change the conclusions of the statistical analyses.

3.0 Results

The summary statistics for the horizontal flux measurements made during sampling periods with and without precipitation are shown in Tables 1 and 2, respectively. A Mann-Whitney test of the differences between these data sets showed that both the grassland and woodland sites had significant increases in horizontal mass flux during periods with precipitation at the sampling height closest to the ground (25 cm [10 in.]). This increase was not seen at the 50 cm and 1 m (20 and 39 in.) sampling heights. These results suggest that rainsplash does contribute to the amount of soil collected in the BSNE samplers, but that these effects are greatest at the lowest sampling heights; rainsplash does not appear to significantly affect the results at sampling heights of 50 cm (20 in.) and above.

Figure 6 shows the measured horizontal mass flux at a 1 m (39 in.) height for all sampling periods at the MDA J grass-covered site (Figure 6a) and at the TA-51 piñon-juniper woodland site (Figure 6b). The horizontal mass flux appears to increase through the spring and early summer months, with more variability in the later summer months. A visual comparison of the graphs indicates that the horizontal mass flux seems to be greater at the grass-covered site than at the woodland site.

Figure 7 compares the horizontal mass flux results by sampling height. The data used in Figure 7 were collected during sampling periods with no precipitation because of the impact of rainsplash on measured dust flux at 25 cm (10 in.). Thus, the figure reflects only the differences in wind-driven dust flux between the grass and woodland cover. Statistical comparisons between the two sites show the horizontal mass flux at the grass-covered site was significantly greater than at the woodland site. This difference in dust flux was likely the result of higher ground-level wind velocities at the grass-covered site. The difference in wind velocities is shown in Figure 8; the average and maximum gust velocities at 1 m (39 in.) above the ground are about two times greater at the more open grass-covered site than at the woodland site.

Figure 9 compares the horizontal mass flux measured by the motion-restricted BSNE samplers facing inward and outward relative to the center of the circular plot. Statistical comparisons of the inward and outward fluxes show no significant difference, regardless of whether precipitation occurred during the sampling period. Thus, the quantity of dust entering the circular sample site was equal to that leaving the sampling site, which suggests no net loss of soil from the area. These findings were consistent at both the grass-covered and woodland sites.

Table 1
Summary Statistics for Horizontal Mass Flux Measurements from All Sampling Periods

Sampling Location	Summary Statistics ($g/m^2/yr$)					No. of Samples
	Mean	Standard Deviation	Median	Minimum	Maximum	
Grass-Covered Site (MDA J)						
Fully Rotating Samplers						
All Heights	1.3E+03	2.9E+03	4.6E+02	0E+00	2.7E+04	324
25 cm	2.5E+03	4.6E+03	7.0E+02	2.9E+01	2.7E+04	108
50 cm	8.3E+02	1.0E+03	4.9E+02	1.8E+01	4.8E+03	108
1 m	4.7E+02	4.9E+02	3.6E+02	0E+00	4.3E+03	108
Motion-Restricted (45°) Samplers						
Inward-Facing	5.8E+02	8.4E+02	3.0E+02	1.1E+01	7.1E+03	216
Outward-Facing	5.1E+02	8.3E+02	2.5E+02	–1.3E+03	6.1E+03	216
Woodland Site (TA-51)						
Fully Rotating Samplers						
All Heights	1.2E+03	5.3E+03	2.7E+02	–4.0E+00	6.8E+04	336
25 cm	2.7E+03	8.9E+03	3.3E+02	–4.0E+00	6.8E+04	112
50 cm	5.9E+02	1.2E+03	2.8E+02	–3.3E+01	9.5E+03	112
1 m	3.0E+02	3.0E+02	2.5E+02	–3.7E+01	2.6E+03	112
Motion-Restricted (45°) Samplers						
Inward-Facing	4.6E+02	9.0E+02	2.4E+02	–2.6E+03	7.0E+03	224
Outward-Facing	4.5E+02	8.5E+02	2.3E+02	–1.2E+01	8.3E+03	224

Table 2
Summary Statistics for Horizontal Mass Flux Measurements from Periods without Precipitation

Sampling Location	Summary Statistics ($g/m^2/yr$)					No. of Samples
	Mean	Standard Deviation	Median	Minimum	Maximum	
Grass-Covered Site (MDA J)						
Fully Rotating Samplers						
All Heights	5.3E+02	3.3E+02	4.4E+02	7.3E+01	2.3E+03	120
25 cm	5.6E+02	3.6E+02	4.6E+02	1.3E+02	1.7E+03	40
50 cm	5.2E+02	2.4E+02	4.5E+02	1.5E+02	1.1E+03	40
1 m	5.0E+02	3.7E+02	3.7E+02	7.3E+01	2.3E+03	40
Motion-Restricted (45°) Samplers						
Inward-Facing	2.8E+02	1.3E+02	2.4E+02	9.5E+01	6.4E+02	80
Outward-Facing	3.2E+02	6.7E+02	2.1E+02	7.7E+01	6.1E+03	80
Woodland Site (TA-51)						
Fully Rotating Samplers						
All Heights	3.9E+02	3.0E+02	3.1E+02	7.3E+01	2.3E+03	76
25 cm	3.3E+02	2.2E+02	2.5E+02	1.6E+02	1.2E+03	36
50 cm	2.6E+02	9.7E+01	2.4E+02	7.3E+01	5.8E+02	36
1 m	2.6E+02	7.8E+01	2.5E+02	1.4E+02	4.3E+02	36
Motion-Restricted (45°) Samplers						
Inward-Facing	2.5E+02	2.6E+02	2.0E+02	7.7E+01	2.3E+03	72
Outward-Facing	2.2E+02	9.3E+01	2.0E+02	–1.2E+02	4.6E+02	72

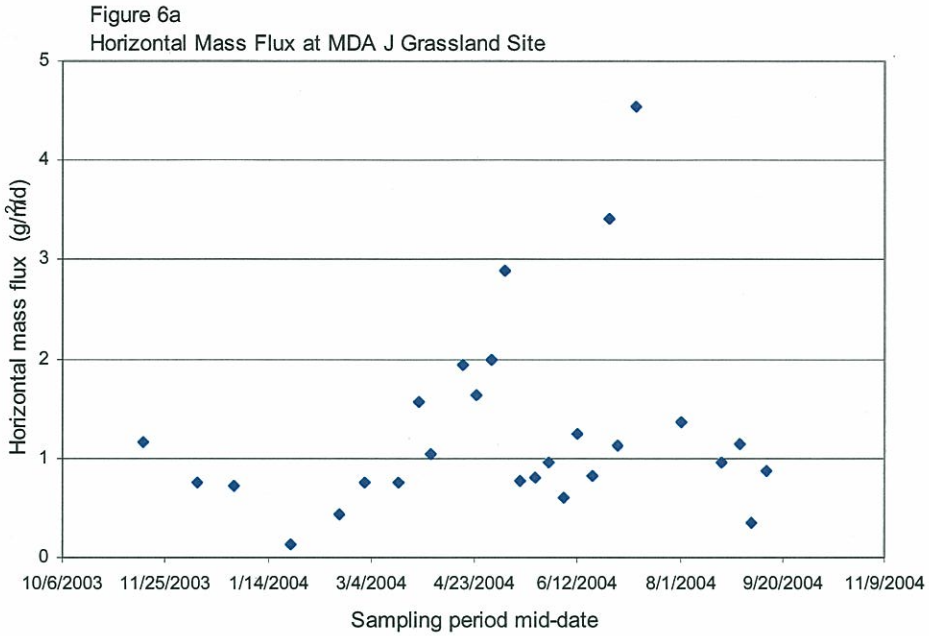

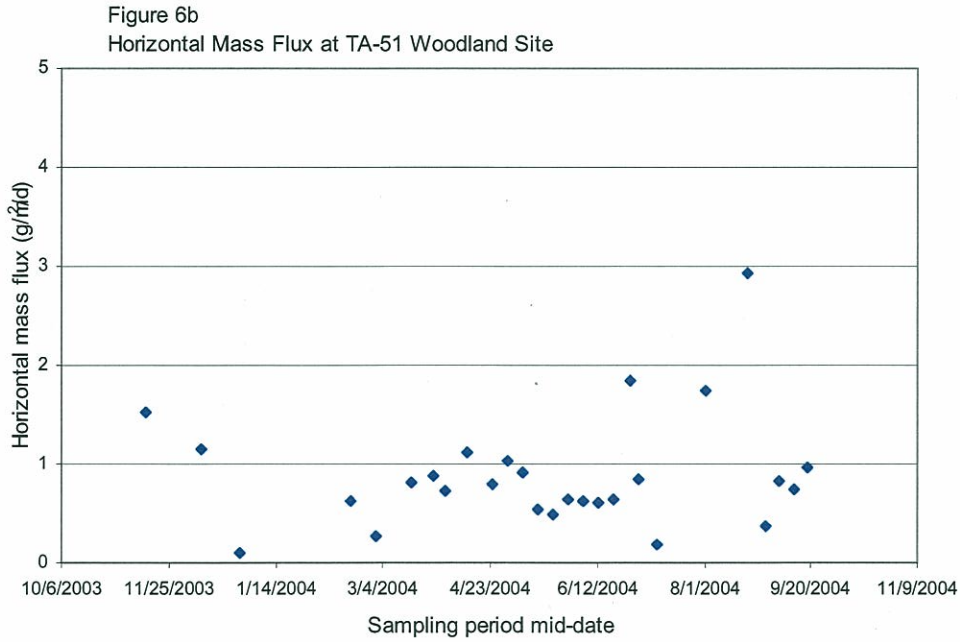

Figure 6
Horizontal Mass Flux at Grassland and Woodland Analog Sites over Time (1 m sampling height)

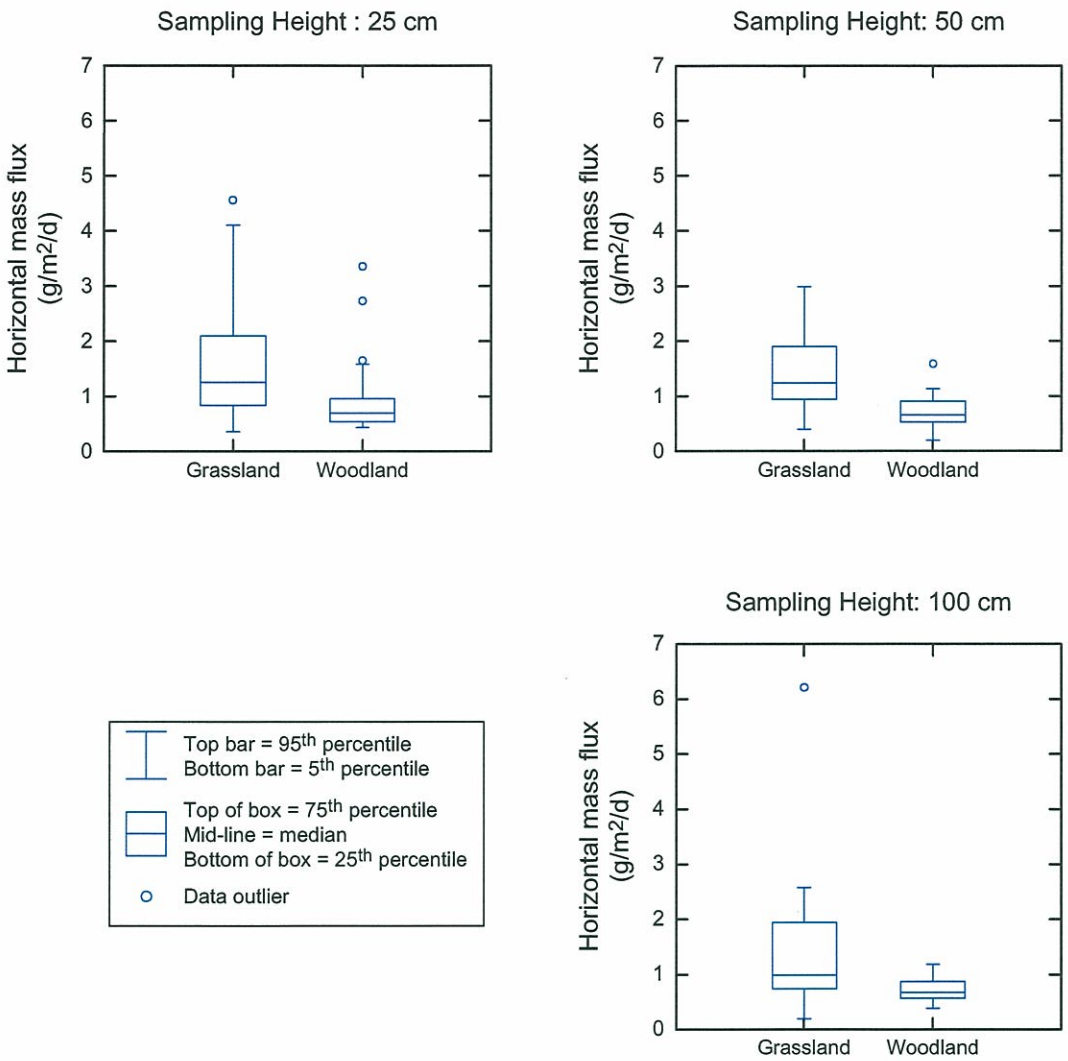

Figure 7
Horizontal Mass Flux at Grassland and Woodland Analog Sites (all sampling heights)

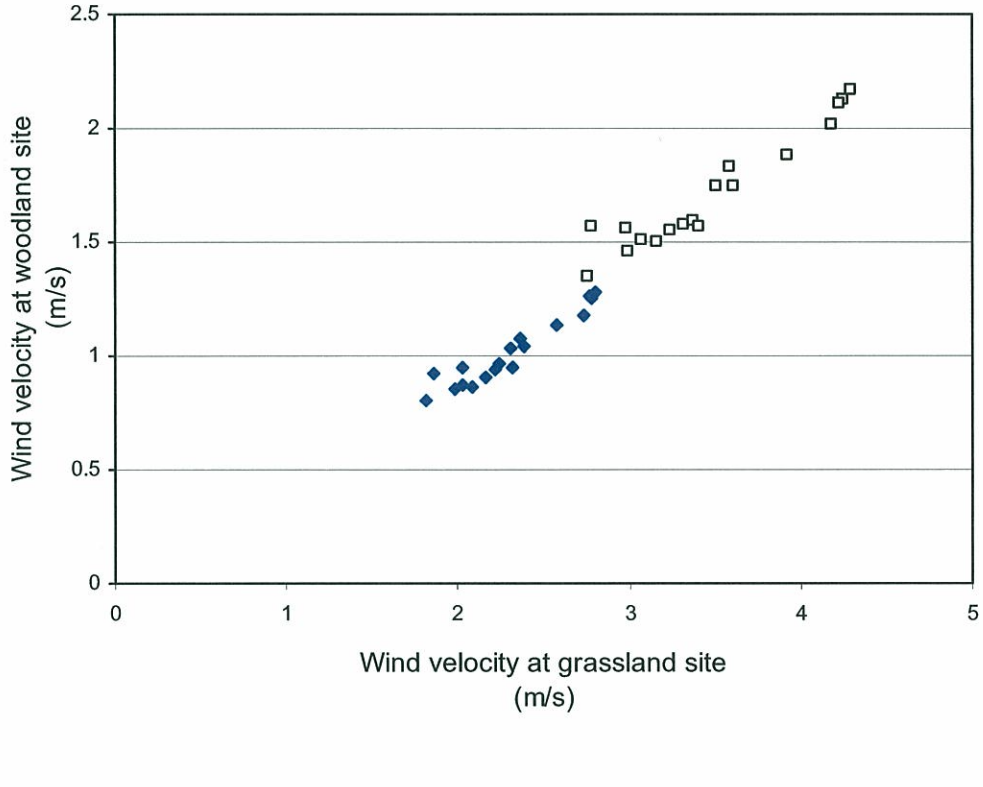

Figure 8
Wind Velocities at Grassland and Woodland Analog Sites
(1 m sampling height)

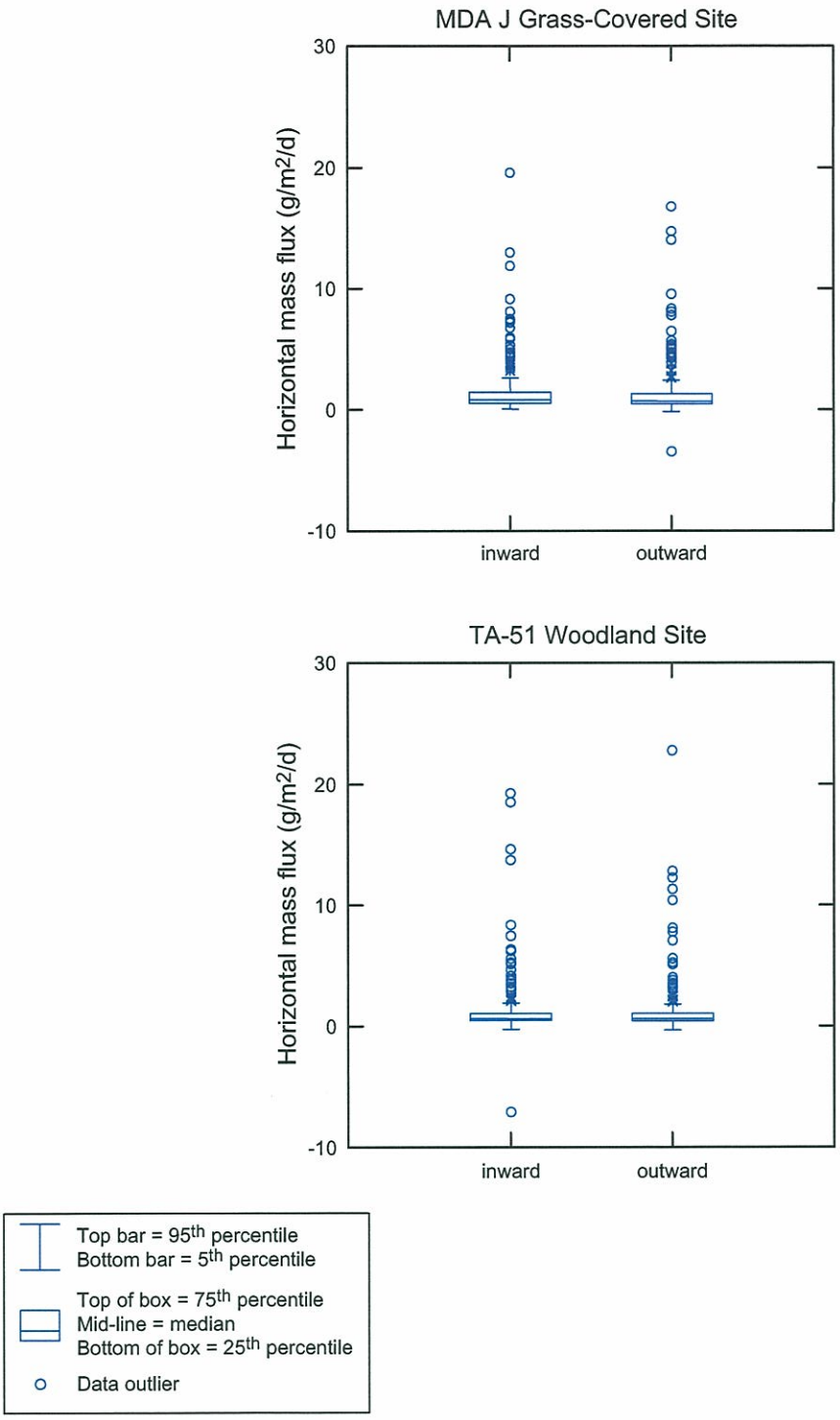

Figure 9
Horizontal Mass Flux at Inward- and Outward-Facing Samplers at Both Analog Sites

While horizontal flux describes saltating dust moving horizontally through an area at lower heights, vertical flux describes dust moving up and down. The particles described by vertical flux are typically smaller in diameter and can be transported for long distances; accordingly, these particles present an off-site risk. Figure 10 shows the range of measured values for the vertical flux. Note that positive numbers represent upward flux (removal from the area) and negative numbers represent downward net flux (deposition within the area). Table 3 shows the summary statistics for aerosol mass concentrations and the vertical flux measurement data. Overall, the average vertical flux at 2 m (6.6 ft) above the soil surface was 2.6 ± 12.3 g/m^2/yr ($5.4 \times 10^{-4} \pm 3.0 \times 10^{-3}$ lb/ft^2/yr) or 0.03 ± 0.12 mT/ha/yr (0.013 ± 0.054 t/ac/yr), which suggests little, if any, net loss from the area from suspended soils.

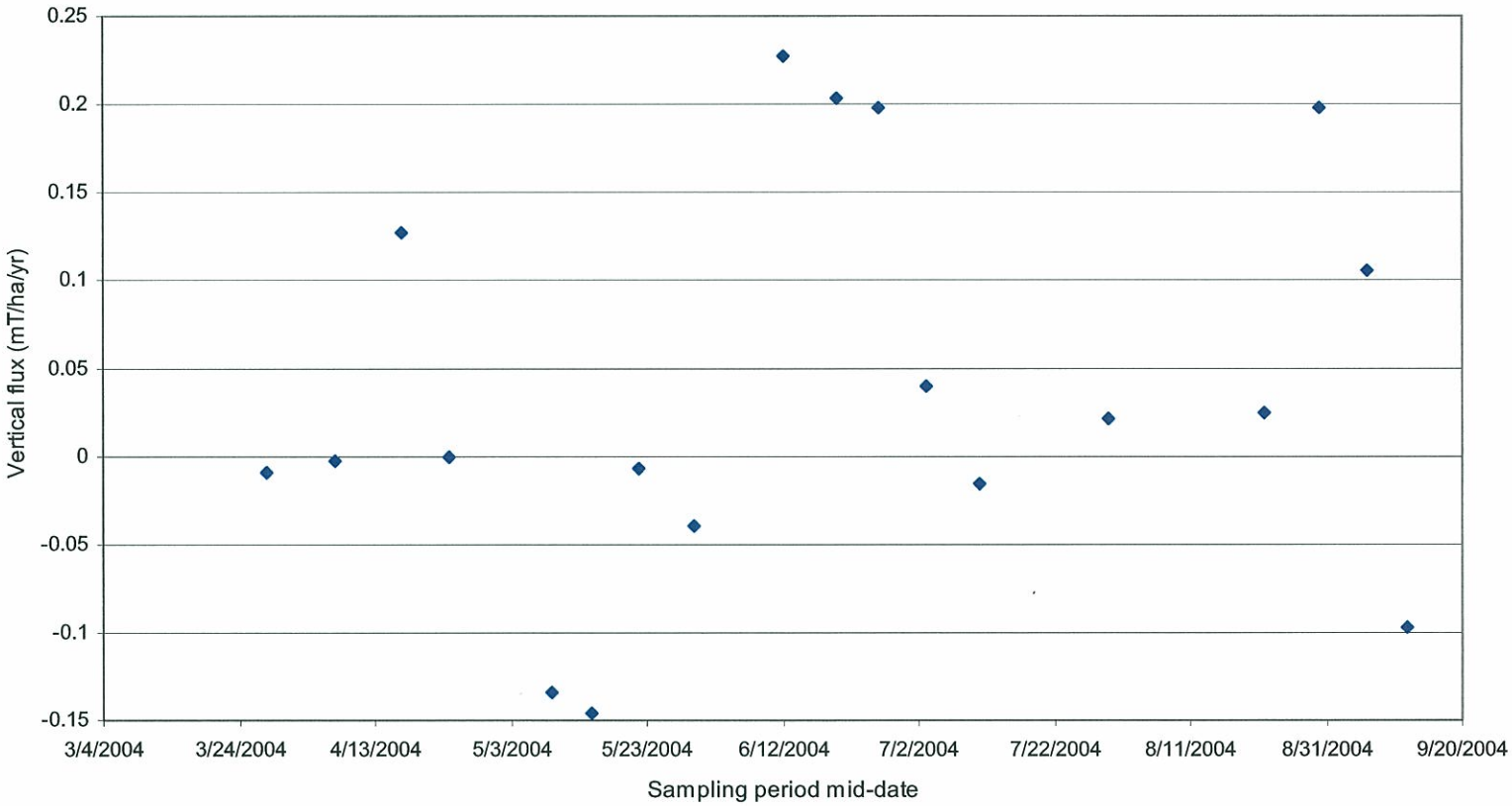

Figure 10
Estimated Vertical Mass Flux Collected during All Sampling Periods (1 m sampling height)

Table 3
Summary Statistics for Aerosol Mass Concentration and Vertical Mass Flux at MDA J

Summary Statistic	Mass Concentration ($\mu g/m^3$) [a]	Vertical Mass Flux ($g/m^2/yr$)	Vertical Mass Flux (mT/ha/yr)
Average	1.1E+01	2.6E+00	3.0E–02
Standard Deviation	1.7E+01	1.2E+01	1.2E–01
Median	1.0E+01	0.0E+00	0.0E+00
Minimum	3.5E+00	–2.0E+01	–2.0E–01
Maximum	2.7E+01	2.3E+01	2.3E–01
Range	2.4E+01	4.3E+01	4.3E–01

[a] *Measurements for aerosol mass concentration averaged over 1 m and 3 m sampling heights for a total of 19 samples.*

4.0 Discussion

This study provides the first known set of wind erosion measurements on a landfill cover. No previous assessment has estimated the effect of wind erosion using data, site-specific or otherwise, on long-term cover performance and associated risks. In fact, there are few data sets on wind erosion for semiarid ecosystems dominated by grass cover, the results for short-grass steppe adjacent to Rocky Flats in Colorado (Breshears et al., 2003) being the one noteworthy exception.

The horizontal transport component of wind erosion was quantified using rotating BSNE samplers. Transport, as noted above, relates to the local movement and redistribution of soil, but does not necessarily reflect net erosion. That is, significant amounts of soil can move into and out of an area, and previous estimates have reflected only relative differences in total horizontal mass flux, not net erosion (Breshears et al., 2003). The study design adopted here used motion-restricted samplers that allowed directional measurements for analysis of net loss due to horizontal transport.

The estimates of vertical flux provide the most direct measurements of wind erosion and suggest a small net loss of soil from the sampling sites over the period studied. The flux measurements presented here are similar to those reported by Breshears et al. (2003), who measured a mean vertical flux of 3.0 $g/m^2/yr$ (0.071 $lb/ft^2/yr$) at a grassland near Denver, Colorado. As seen in previous studies (Whicker et al., 2002; Breshears et al., 2003), wind erosion is highly variable temporally within the one- to two-week intervals studied. The results of this study provide distributions that describe this temporal variability for the period studied.

4.1 Significance of Results

As seen in previous studies (Breshears et al., 2003), horizontal wind transport greatly exceeds net soil loss, by more than two orders of magnitude for some conditions and heights. The results of the current study suggest that horizontal wind-driven dust flux is frequently moving material into and out of the area, resulting in a small net erosional loss accumulated over the course of the study. The additional data from the circular design reinforce this interpretation: the net flux into and out of the circular area were not significantly different. Because this study quantifies all three components of dust-flux, it provides a higher degree of confidence about interpreting wind-driven processes than is feasible with less robust studies.

The wind-driven transport and erosion data set in the woodland site is also unique. Only a few measurements of soil erosion have been reported for a woodland setting (Baker and Jemison, 1991), and those data estimate only horizontal transport rates; they do not provide information on site conditions or estimates of uncertainty or variance. Not surprisingly, the present study

showed that horizontal wind-driven dust fluxes in the woodland site (TA-51) were lower than those at the grass-covered (MDA J) site. This is consistent with the findings of Breshears et al. (2003), who found horizontal fluxes in grassland were about an order of magnitude greater than those in woodlands. In each case, the rough, heterogeneous canopy structure associated with the woodland has a major effect on the boundary layer and surface roughness, and these factors, in turn, affect wind dynamics and associated soil transport and erosion. In addition, data from the circular sampling area at the woodland site indicate no significant net gain or loss of soil (i.e., the amounts of dust being deposited into and removed from the study area are essentially the same). Again, this indicates that, despite the fairly substantial amount of transport occurring at the site, overall net loss of soil cover is relatively low.

The data collected in this study can be used to provide parameters for models used to assess long-term cover performance and associated risks. Also, the wind erosion estimates can be compared against the estimates of water erosion being developed for MDA G to assess the relative magnitude of the two processes.

Wind erosion is important at MDA G in two contexts, both of which should be considered. First, wind erosion should be factored into estimations of long-term cover integrity. Second, even if water erosion proves to be the dominant force for degradation of the landfill, wind-driven transport may be the most important risk pathway for any exposed contamination. Such contamination might result from erosional loss of the cover or from biological intrusion into the waste caused by burrowing animals or plant root uptake.

4.2 Qualifications

Although the results reported above are useful for assessing the long-term performance of MDA G, a number of qualifications apply to the findings:

1. The data reported here cover only part of a year. Improved estimates would be obtained if the measurements were made over a minimum of a full year. Year-to-year variation is also of concern (Breshears et al., 2003) and multiyear estimates would provide even more confidence for longer-term extrapolations.

2. Correlation of wind transport and erosion to wind conditions is currently limited to one- to two-week intervals because of limits imposed by the need to collect and weigh dust. However, new automated systems for measuring dust flux could provide a basis for developing more predictive relationships between wind distributions and wind erosion.

3. Two vegetation scenarios were evaluated in this study: MDA J as an analog for immediate postclosure conditions at MDA G and the TA-51 woodland site as a later

successional analog. There is, however, considerable uncertainty about the actual ecological trajectory that vegetation will follow at MDA G. This trajectory will, of course, be influenced by climate. Periods of drought could lead to loss of ground cover through mortality and fire. Indeed, such changes have driven the dominant vegetation and soil erosion dynamics around Los Alamos for the past several decades, most notably through the 1950s drought, the Cerro Grande Fire of 2000, and the tree-killing drought of the new millennium (2000 to 2004) (Breshears and Allen, 2002; Allen and Breshears, 1998; Davenport et al., 1998). Disturbances such as fire result in major increases in wind and water erosion and associated contaminant transport (Whicker et al., 2002, Johansen et al., 2001a, 2001b, 2003). The estimates presented here do not account for such probable events, which are of increased likelihood due to global change (Breshears and Allen, 2002).

Anthropogenic disturbances can also have tremendous impacts on soil erosion. For example, Figures 11 and 12 illustrate how wind erosion at a site just east of MDA G, but within the TA-54 boundary, increased following tree-thinning operations in the nearby piñon-juniper woodland. Figure 11 shows aerosol mass concentrations before and after tree thinning and Figure 12 shows that the flux gradient changed from neutral (no net loss) to one of sustained soil loss following tree thinning. Clearly, ecosystem disturbance through anthropogenic management of the vegetation cover can dramatically alter soil erosion rates over short periods of time; the effects of these disturbances may persist over longer periods of time, depending on how long it takes the ecosystem to recover.

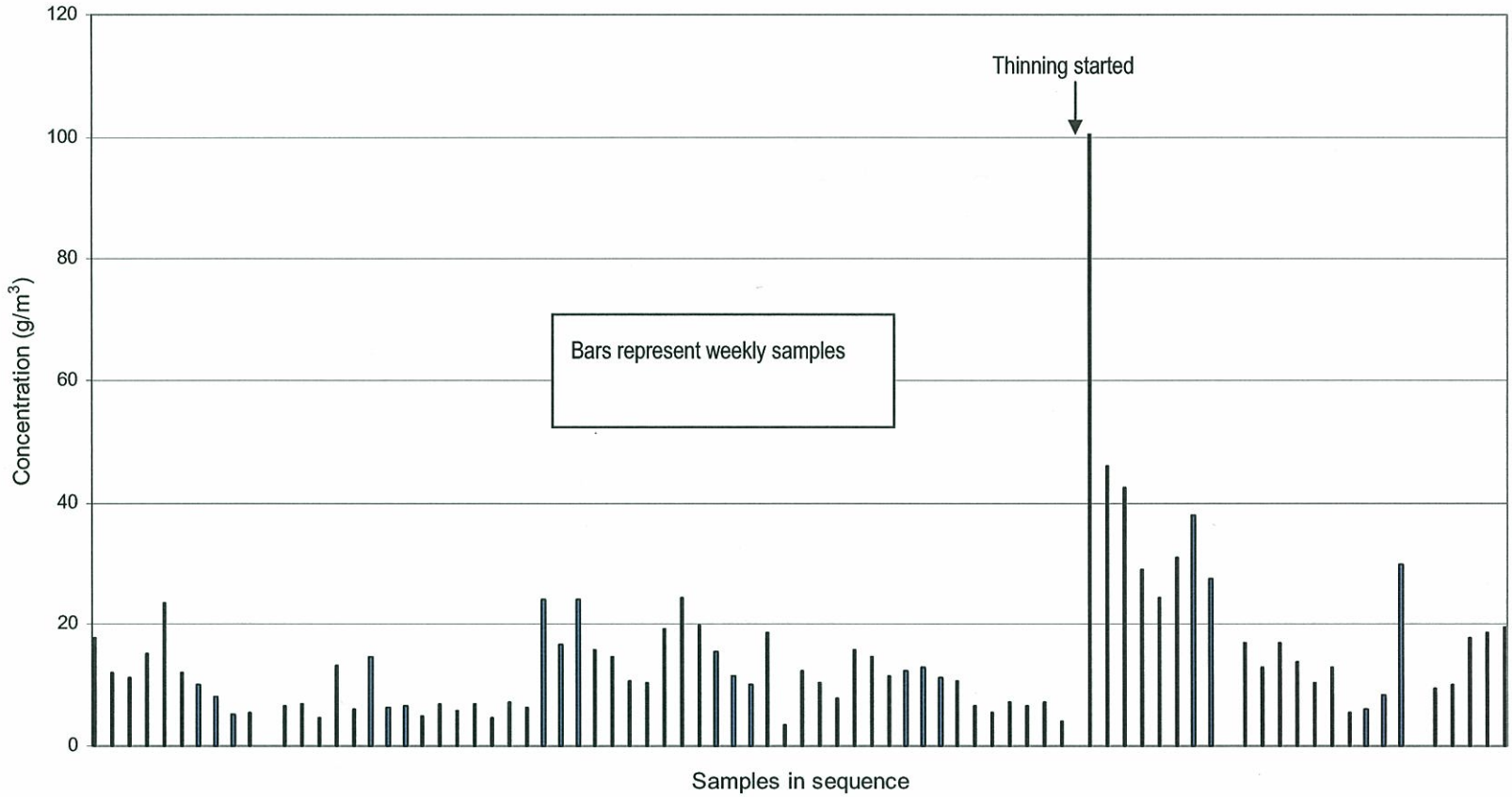

Figure 11
Pre- and Post-Thinning Dust Concentrations at TA-54 Meteorological Station

Source: Whicker et al., 2003

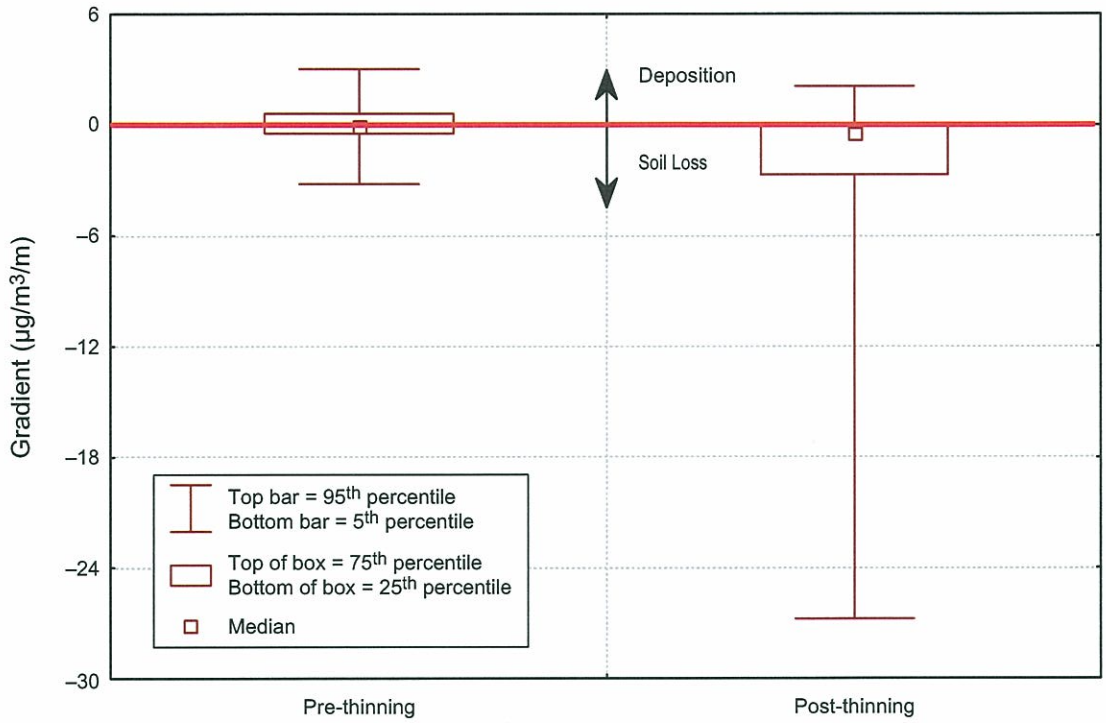

Figure 12
Weekly Flux Gradient Measurements at TA-54 before and after Nearby Thinning Operations

Source: Whicker et al., 2003

5.0 References

Allen, C.D., and D.D. Breshears, 1998, "Drought-Induced Shift of a Forest-Woodland Ecotone: Rapid Landscape Response to Climate Variation," *Proceedings of the National Academy of Sciences USA,* Vol. 95, pp. 14,839–14,842.

Anspaugh, L.R., J.H. Shinn, P.L. Phelps, and N.C. Kennedy, 1975, "Resuspension and Redistribution of Plutonium in Soils," *Health Physics*, Vol. 29, pp. 571–582.

Arimoto R., T.B. Kirchner, J. Webb, M. Conley, B. Stewart, D. Schoep, and M. Walthall. 2002. "239, 240Pu and Inorganic Substances in Aerosols from the Vicinity of the Waste Isolation Pilot Plant: The Importance of Resuspension," *Health Physics*, Vol. 83, pp. 456–470.

Bagnold, R.A., 1941, *The Physics of Blown Sand and Desert Dunes*, Chapman and Hall Ltd., London.

Baker M.B. Jr., R.L. Jemison, 1991, "Soil Loss—Key to Understanding Site Productivity," *Proceedings of 36th Annual New Mexico Water Conference–Agencies and Science Working for the Future, 1991 November 7–8*, New Mexico Water Resources Research Institute Report No. 265, New Mexico Water Resources Research Institute, Las Cruces, New Mexico.

Breshears, D.D., C.D. Allen, 2002, "The Importance of Rapid, Disturbance-Induced Losses in Carbon Management and Sequestration," *Global Ecology and Biogeography*, Vol. 11, pp. 1–5.

Breshears, D.D., J.J. Whicker, M.P. Johansen, and J.E. Pinder, 2003, "Wind and Water Erosion and Transport in Semi-Arid Shrubland, Grassland, and Forest Ecosystems: Quantifying Dominance of Horizontal Wind-Driven Transport," *Earth Surface Processes and Landforms*, Vol. 28, pp. 1,189–1,209.

Campbell Scientific Canada Corp., 2004, *3-D Sonic Anemometer, Model CSAT3*, Brochure printed January 2004. <http://www.campbellsci.ca/CampbellScientific/Catalogue/CSAT3_Br.pdf>.

Davenport, D.W., D.D. Breshears, B.P. Wilcox, and C.D. Allen, 1998, "Viewpoint: Sustainability on Piñon-Juniper Ecosystems: A Unifying Perspective on Soil Erosion Thresholds," *Journal of Range Management*, Vol. 51, pp. 231–240.

Fryrear, D.W., 1985, "Soil Cover and Wind Erosion," *Transactions of ASAE*, Vol. 28, pp. 781–784.

Fryrear, D.W., 1986, "A Field Dust Sampler," *Journal of Soil and Water Conservation*, Vol. 41, pp. 117–120.

Gillette, D.A, D.W. Fryrear, J.B. Xiao, P. Stockton, D. Ono, P.J. Helm, T.E. Gill, and T. Ley, 1997, "Large-Scale Variability of Wind Erosion Mass Flux Rates at Owens Lake: Vertical

Profiles of Horizontal Mass Fluxes of Wind-Eroded Particles with Diameter Greater than 50 μm," *Journal of Geophysical Research,* Vol. 102(D22), pp. 25,977–25,987.

Goossens, D. and Z.Y. Offer, 2000, "Wind Tunnel and Field Calibration of Six Aeolian Dust Samplers," *Atmospheric Environment*, Vol. 34, pp. 1,043–1,057.

Johansen, M.P., T.E. Hakonson, and D.D. Breshears, 2001a, "Post-Fire Runoff and Erosion from Rainfall Simulation: Contrasting Forests with Shrublands and Grasslands, *Hydrologic Processes*, Vol. 15, pp. 2,953–2,965.

Johansen, M.P., T.E. Hakonson, F.W. Whicker, R.J. Simanton, and J.J. Stone, 2001b, "Hydrologic Response and Radionuclide Transport Following Fire at Semiarid Sites," *Journal of Environmental Quality*, Vol. 30(6), pp. 2,010–2,017.

Johansen, M.P., T.E. Hakonson, F.W. Whicker, and D.D. Breshears, 2003, "Pulsed Redistribution of a Contaminant Following Forest Fire: Cs-137 in Runoff," *Journal of Environmental Quality,* in press.

Liu, B.Y.H. and Y.H. Pui, 1981, "Aerosol Sampling Inlets and Inhalable Particles," *Atmospheric Environment*, Vol. 15, pp. 589–600.

Nyhan, J.W., L.W. Hacker, T.E. Calhoun, and D.L. Young, 1978, *Soil Survey of Los Alamos County, New Mexico*, Los Alamos National Laboratory Report LA-677-MS.

Rodgers, J.C., P.T. Wasiolek, J.J. Whicker, C. Eberhart, K. Saxton, and D. Chandler, 2000, *Performance Evaluation of LANL Environmental Radiological Air Monitoring Inlets at High Wind Velocities Associated with Resuspension*, Los Alamos National Laboratory Report LA-UR-00-3091.

Sehmel, G.A., 1980, "Particle Resuspension: A Review," *Environment International*, Vol. 4, pp. 107–127.

Stout, J.E. and T.M. Zobeck, 1996, "The Wolfforth Field Experiment: A Wind Erosion Study," *Soil Science*, Vol. 161, pp. 616–632.

Stull, R.B., 1988, *An Introduction to Boundary Layer Meteorology*, Kluwer Academic Publishers, The Netherlands.

Webb, S.B., S.A. Ibrahim, and F.W. Whicker, 1997, "A Three-Dimensional Spatial Model of Plutonium in Soil Near Rocky Flats, Colorado," *Health Physics*, Vol. 73(2), pp. 340–349.

Whicker, J.J., D.D. Breshears, P.T. Wasiolek, T.B. Kirchner, R.A. Tavani, D. Schoop, and J. Rodgers, 2002, "Temporal and Spatial Variation of Episodic Wind Erosion in Unburned and Burned Shrubland," *Journal of Environmental Quality*, Vol. 31, pp. 599–612.

Whicker J.J., J.E. Pinder, and D.D. Breshears, 2003, "Increased Contaminant Transport Following Wildfire," presented at the Annual Health Physics Society, *Health Physics* Vol. 84, pp. S206.